Electronic properties of STM-constructed dangling-bond dimer lines on a Ge(001)-(2×1):H surface

Marek Kolmer,[1] Szymon Godlewski,[1,*] Hiroyo Kawai,[2,†] Bartosz Such,[1] Franciszek Krok,[1] Mark Saeys,[2,3] Christian Joachim,[2,4] and Marek Szymonski[1]

[1]*Department of Physics of Nanostructures and Nanotechnology, Institute of Physics, Jagiellonian University, Reymonta 4, PL 30-059 Krakow, Poland*

[2]*Institute of Materials Research and Engineering, 3 Research Link, Singapore 117602, Singapore*

[3]*Department of Chemical and Biomolecular Engineering, National University of Singapore, 4 Engineering Drive 4, Singapore 117576, Singapore*

[4]*Nanosciences Group & MANA Satellite, CEMES-CNRS, 29 rue Jeanne Marvig, F-31055 Toulouse, France*

(Received 25 April 2012; revised manuscript received 3 August 2012; published 6 September 2012)

Atomically precise dangling-bond (DB) lines are constructed dimer-by-dimer on a hydrogen-passivated Ge(001)-(2×1):H surface by an efficient scanning tunneling microscope (STM) tip-induced desorption protocol. Due to the smaller surface band gap of the undoped Ge(001) substrate compared to Si(001), states associated with individually created DBs can be characterized spectroscopically by scanning tunneling spectroscopy (STS). Corresponding dI/dV spectra corroborated by first-principle modeling demonstrate that DB dimers introduce states below the Ge(001):H surface conduction band edge. For a DB line *parallel* to the surface reconstruction rows, the DB-derived states near the conduction band edge shift to lower energies with increasing number of DBs. The coupling between the DB states results in a dispersive band spanning 0.7 eV for an infinite DB line. For a long DB line *perpendicular* to the surface reconstruction rows, a similar band is not formed since the interdimer coupling is weak. However, for a short DB line (2–3 DBs) perpendicular to the reconstruction rows a significant shift is still observed due to the more flexible dimer buckling.

DOI: 10.1103/PhysRevB.86.125307 PACS number(s): 73.20.At, 68.37.Ef

I. INTRODUCTION

Silicon Si(001):H and germanium Ge(001):H hydrogen-passivated surfaces are promising platforms for the atomic-scale fabrication of mesoscopic electronic devices[1] and for the construction of atomic-scale surface electronic circuits.[2,3] The desorption of surface hydrogen atoms using the scanning tunneling microscope (STM) tip creates very localized dangling-bond (DB) electronic states within the surface band gap of those materials.[1,4–8] These nanostructures can be used as interconnects in molecular electronics devices stabilized on a surface,[9] create DB logic circuits based on quantum interferences,[2] or act as qubits for the surface miniaturization of quantum computers.[6–8] The formation of single, double DBs,[10–19] and long DB lines[3,4,20] on a Si(001):H surface, as well as selective *in situ* doping by PH_3 gas has been studied by STM techniques both at room temperature and at low temperatures (LT).[1,5,8,20–22] Although it has been theoretically predicted that DB lines running parallel and perpendicular to the Si(001):H dimer rows will have very different electronic transport properties,[23,24] those properties have not yet been characterized spectroscopically. It is important to quantify the difference between the DB lines in both directions in order to design efficient atomic-scale devices using DBs.[2] Specifically, it is crucial to determine the maximum and minimum length of DB line interconnects between surface molecular devices,[9] as well as to investigate the surface tunneling leakage current[24] in both directions. However, due to the larger surface band gap, it is challenging to spectroscopically characterize the states introduced by DB nanostructures in the surface band gap of Si(001):H. As we demonstrate in this paper, the smaller surface band gap of Ge(001):H makes it possible to precisely track the gradual shift in the energy levels of the DB states as a function of number of DBs using scanning tunneling spectroscopy (STS), as DB lines are created dimer-by-dimer.

We report an efficient STM protocol to construct predesigned DB nanostructures on a Ge(001):H surface. First, short atomic lines containing 1–5 DB dimers are fabricated. Near the bottom of the Ge(001):H surface conduction band edge, the progressive introduction of DB electronic states is studied using LT-STM dI/dV spectroscopy. Short DB dimer lines introduce electronic states in the gap. Those states can be used to design DB logic gates.[2] When the length of DB lines increases beyond 3 DB dimers, a conduction channel gradually develops below the bottom of the Ge(001):H conduction band edge for DB lines parallel to the reconstruction rows.

II. EXPERIMENTAL AND COMPUTATIONAL DETAILS

The Ge samples used in the STM/STS measurements were cut from undoped Ge(001) wafers (TBL Kelpin Crystals, n-type, ∼45 Ω cm). After insertion into the UHV system, the samples were first sputtered and annealed for 15 min (Ar^+, 600 eV, 1020 K). The sputtering cycles were repeated until a clean $c(4\times2)/p(2\times2)$ surface was obtained as confirmed by low energy electron diffraction (LEED) and LT-STM measurements. Then hydrogen passivation was performed using a home-built hydrogen cracker to provide atomic hydrogen. During the passivation procedure, the samples were kept at 485 K and the hydrogen pressure was maintained at 1×10^{-7} mbar. The base pressure of the STM chamber was in the low 10^{-10} mbar range. All STM/STS measurements were performed at 5 K (liquid helium). Before construction of the DB dimer lines, the bare Ge(001) and Ge(001):H surface structures were characterized by comparing the experimental and calculated STM images. The electronic properties of DB dimer

 ©2012 American Physical Society

lines were analyzed in detail using density functional theory (DFT) surface electronic structure calculations and dI/dV spectra calculated using the surface Green-function matching (SGFM) method.[25] The STM images and dI/dV spectra were calculated for structures optimized using DFT[26] with the Perdew-Burke-Ernzerhof (PBE) functional,[27] as implemented in the Vienna *ab initio* simulation package (VASP) (see Appendix A). STM images were calculated using the SGFM method[25] with an extended Huckel molecular orbital (EHMO) Hamiltonian. The parameters in the EHMO Hamiltonian were fitted to accurate DFT band structures. The HSE06 functional was used to fit the parameters since it provides a more accurate description of the Ge band gap than the PBE functional (see Appendix A). The STM junction was modeled as a semi-infinite W(111) slab, a Ge-terminated STM tip, a nine-layer Ge(001):H surface with the DB nanostructures, and the semi-infinite Ge(001) bulk, as illustrated in Fig. 9. Our approach takes into account the coupling between the surface and the tip and their couplings to the bulk electronic states. This approach provides a realistic description of the ballistic electron transport across the STM junction, while minimizing the computational cost.

III. RESULTS AND DISCUSSION

Starting from a Ge(001):H surface, atomically controlled H extractions were performed by pulsing the STM tip bias voltage. First, the tip was approached over the hydrogen dimer selected for extraction with the STM feedback loop set on a $I = 1$ nA tunneling current intensity and a $V = -0.5$ V bias voltage. The tip apex was positioned over the dimer according to the Ge(001):H filled-state STM image [see Fig. 1(a)]. Subsequently, the feedback loop was turned off and the desorption process started with a V pulse set up at $+1.6$ V. The desorption of the hydrogen dimer was detected when a sudden rise of the tunneling current was observed in the $I(t)$ characteristic. The procedure was repeated step-by-step until the targeted DB dimer pattern was constructed. The above protocol allows for the efficient construction of a predesigned DB nanostructure with atom-by-atom precision, unlike methods based on a fast tip movement along surface dimer rows at a constant speed.[3,4,20] Figure 1 illustrates an atomically controlled dimer-by-dimer desorption leading to the construction of a short 2 DB dimer line parallel to the Ge(001):H rows. Here, unlike in the case of the Si(001):H surface, our STM tip V pulse protocol extracts a pair of H atoms per pulse instead of a single H.

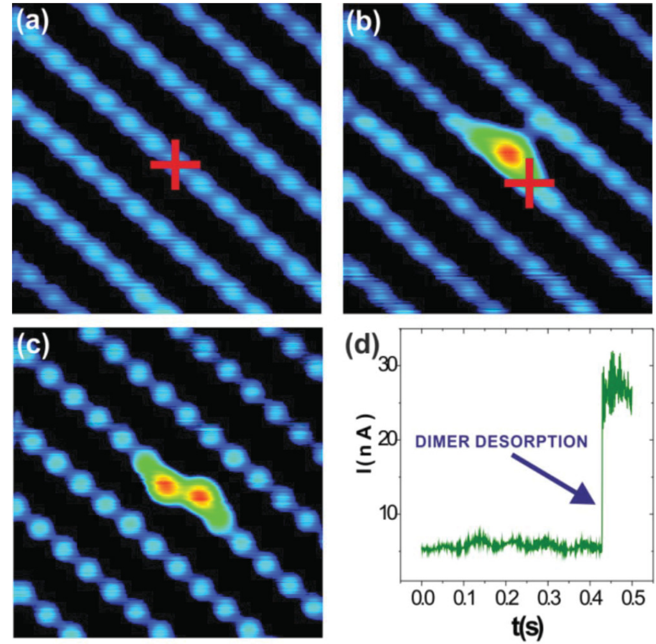

FIG. 1. (Color online) STM tip induced fabrication of a DB line running along the surface reconstruction rows. Red crosses indicate the positions of the tip during the dimer desorption processes: (a) filled-state STM image (−0.5 V, 1 nA, 4 nm × 4 nm) of the hydrogenated Ge(001) surface before desorption, (b) single DB dimer, (c) two neighboring DB dimers forming the DB line, and (d) typical $I(t)$ characteristic recorded during the desorption process.

Following this protocol, short lines consisting of 1 to 3 DB dimers were constructed in both directions, as presented in Fig. 2 (left column). DFT calculations show that infinite DB lines perpendicular and parallel to the Ge(001):H rows buckle by 0.81 and 0.89 Å, respectively. Along the perpendicular direction, the buckling of DB dimers is similar to the buckling of an isolated DB dimer, and in-phase buckling (a down-up-down-up sequence) is more stable than out-of-phase buckling (a down-up-up-down sequence) by 20 meV/dimer. The small energy difference suggests that the buckling is rather flexible for the perpendicular direction. For DB lines parallel to the Ge(001):H rows, out-of-phase buckling, where neighboring DB dimers are buckled in opposite directions, as it is in the $c(4\times2)$ and $p(2\times2)$ reconstructions of the bare Ge(001) surface, is more stable than in-phase buckling, where neighboring DB dimers are buckled in the same direction, by 120 meV/dimer. The calculated STM images for short lines of 1, 2, and 3 DB dimers in both directions [Fig. 2, second column] agree well with the experimental STM images [Fig. 2, first column]. In order to compare the images in more detail, the corrugations over the DBs were also plotted. As presented in Fig. 2 (third column), each calculated constant current line scan agrees well with the corresponding experimental line scan. The small differences in the corrugations can be attributed to details of tip apex electronic structure, as well as to differences in buckling between short and infinite DB lines. The detailed comparison between experimental and calculated STM images furthermore highlights the different surface atomic structure of DB dimer lines constructed on a Ge(001):H surface and on a Si(001):H surface. As reported by Bellec *et al.*, isolated DB dimers do not appear buckled on a Si(001):H surface.[12]

To characterize the electronic properties of each surface, the electronic band structures of the Ge(001):H surface and of the bare Ge(001) surface were calculated [Fig. 3]. The fully hydrogenated Ge(001):H surface is predicted to have a 1.1 eV surface electronic band gap, while the bare Ge(001) surface has a 0.6 eV surface band gap [Figs. 3(a) and 3(d), respectively]. The Ge(001):H surface gap decreases when DB dimer lines are created on the surface due to the electronic states introduced by the DB dimers near the bottom of the Ge(001):H conduction band edge. These bands result from the antibonding π^* states of the Ge(001) DB dimers. The corresponding bonding π states are located well below the top of the valence band

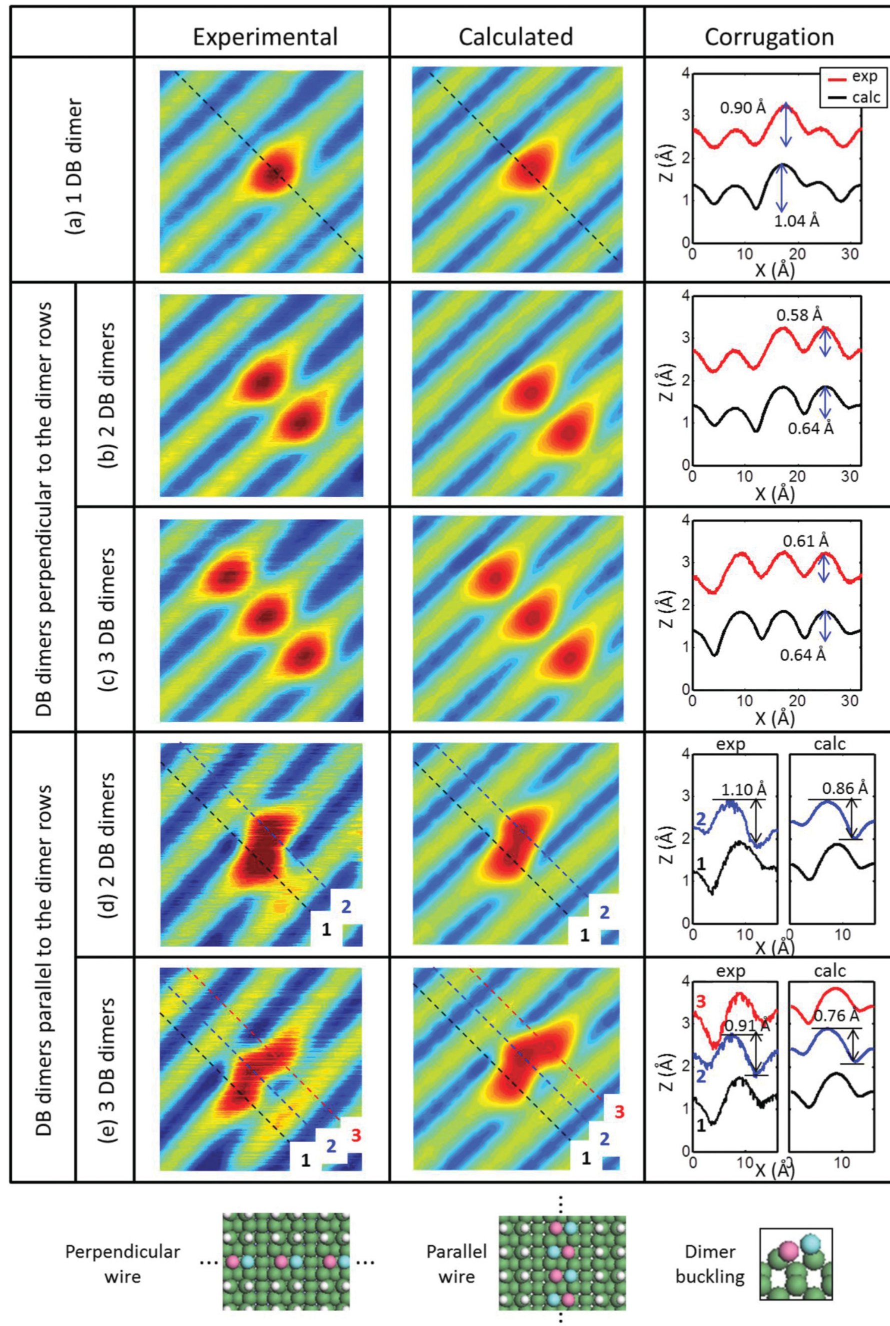

FIG. 2. (Color online) Experimental and calculated STM images of the Ge(001)-(2×1):H surface with (a) 1 DB dimer, (b) and (c) 2 and 3 DB dimers aligned perpendicular to the dimer rows, and (d) and (e) 2 and 3 DB dimers aligned parallel to the dimer rows. The corrugations over the DB dimers are also shown for each case. All STM images acquired at −0.5 V, 1.0 nA, 3 nm × 3 nm. The atomic structures of the DB line perpendicular and parallel to the dimer rows are shown to illustrate the line directions.

edge, and they do not affect the width of the band gap. The band structures for infinite DB lines on Ge(001):H in both the perpendicular and the parallel direction are shown in Figs. 3(b) and 3(c), respectively. In both cases, a new π^* conduction band is created near the bottom of the Ge(001):H conduction band. A significant dispersion of 0.67 eV is however only found for the parallel DB dimer line [Fig. 3(c)].

To investigate how the DB dimer states shift gradually in the Ge(001):H surface band gap as the length of DB line increases, dI/dV spectra were measured and transmission spectra $T(E)$ were calculated for DB lines with various lengths. All STS measurements were performed in a mode with the feedback loop turned on between every two $I(V)$ characteristics to determine the tip position. The $I(V)$ characteristics were automatically collected using a grid covering a 2.5 nm × 2.5 nm surface area, and the corresponding dI/dV spectra were obtained by differentiating the $I(V)$ curves averaged previously over the area of the DBs only. The dI/dV spectra were simulated by calculating the electronic transmission spectra through the tunnel junction used for the constant current image calculations [Fig. 2], which consists of the W tip, the Ge tip apex, the Ge(001):H surface, and the Ge(001) bulk [see Appendix A, Fig. 9]. The tip apex was placed 7 Å above the Ge(001):H surface.

First, the dI/dV spectra for the bare Ge(001) surface and for the fully hydrogenated Ge(001):H surface were measured and compared with calculated $T(E)$ spectra. The experimental dI/dV spectra clearly show that the surface band gap increases upon surface hydrogenation from 0.25 eV for the bare Ge(001) surface to about 0.85 eV for Ge(001):H [light blue and green

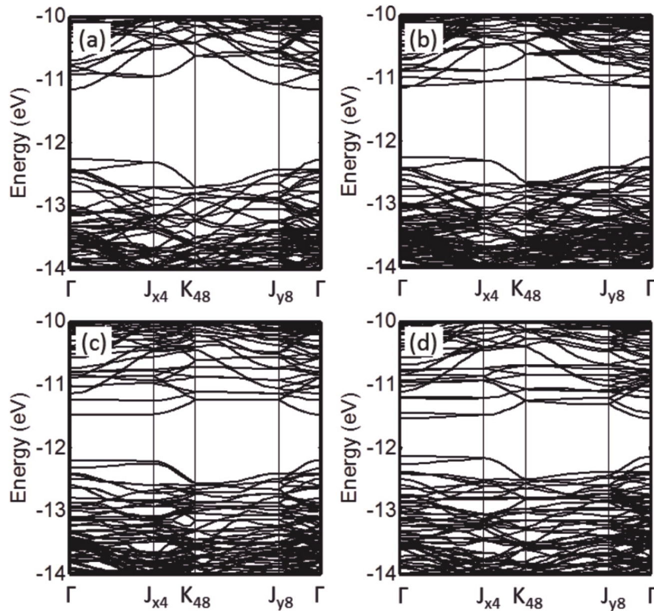

FIG. 3. Band structures of (a) a fully passivated Ge(001)-(2×1):H surface, (b) infinite DB line perpendicular to the dimer rows with seven H-passivated dimers between two DB lines, (c) infinite DB line parallel to the dimer rows, where the DB dimers are buckled out-of-phase along the dimer row, and (d) a clean Ge(001)-$c(4\times2)$ surface. A nine-layer slab was used to model the Ge surfaces.

curves in Fig. 4(a), respectively]. The calculated $T(E)$ spectra [Fig. 4(b)] follow the same trend, in agreement with the calculated bare Ge(001)-$c(4\times2)$ and Ge(001):H surface band structures [Figs. 3(a) and 3(d), respectively]. The band gap for the dI/dV and $T(E)$ spectra differs slightly from the calculated band structures, because a nine-layer slab was used for the band structure calculations while a semi-infinite structure was used in the transport calculations. Note that $T(E)$ was calculated for a single point instead of averaging over the DB area. Therefore, the relative heights and widths of the $T(E)$ resonance peaks are different from the experimental dI/dV spectra.

Next, experimental dI/dV spectra and calculated $T(E)$ spectra are compared for DB lines with 1, 2, 3, and 5 DB dimers in both the perpendicular and the parallel direction. For DB lines in both directions, the experimental dI/dV spectra and the calculated $T(E)$ spectra show large nonzero conductances at energies below the Ge(001):H surface conduction band edge [Fig. 4]. Although these nonzero conductances are found within the Ge(001):H surface gap, they can be detected in the measurements and in the calculations because the Ge bulk band gap is smaller than the 0.85 eV Ge(001):H surface band gap. Note that a large resonance peak appears 0.9 eV above the Fermi level even for a single DB dimer [blue resonance, Figs. 4(a) and 4(c)], clearly showing the DB dimer state introduced below the conduction band edge. This single DB dimer resonance peak is also described well by the calculations [blue resonance peak, Figs. 4(b) and 4(d)]. No resonance peaks are observed near the valence band edge.

For DB lines parallel to the dimer rows, it is expected that the dI/dV resonances are observed below the conduction band edge, and that the resonances will gradually span the 0.6 eV energy difference between the Ge(001):H and the bare Ge(001) conduction band edge as the length of the DB line increases. This is because each DB dimer introduces an additional π^* state near the bottom edge of the Ge(001):H conduction band,

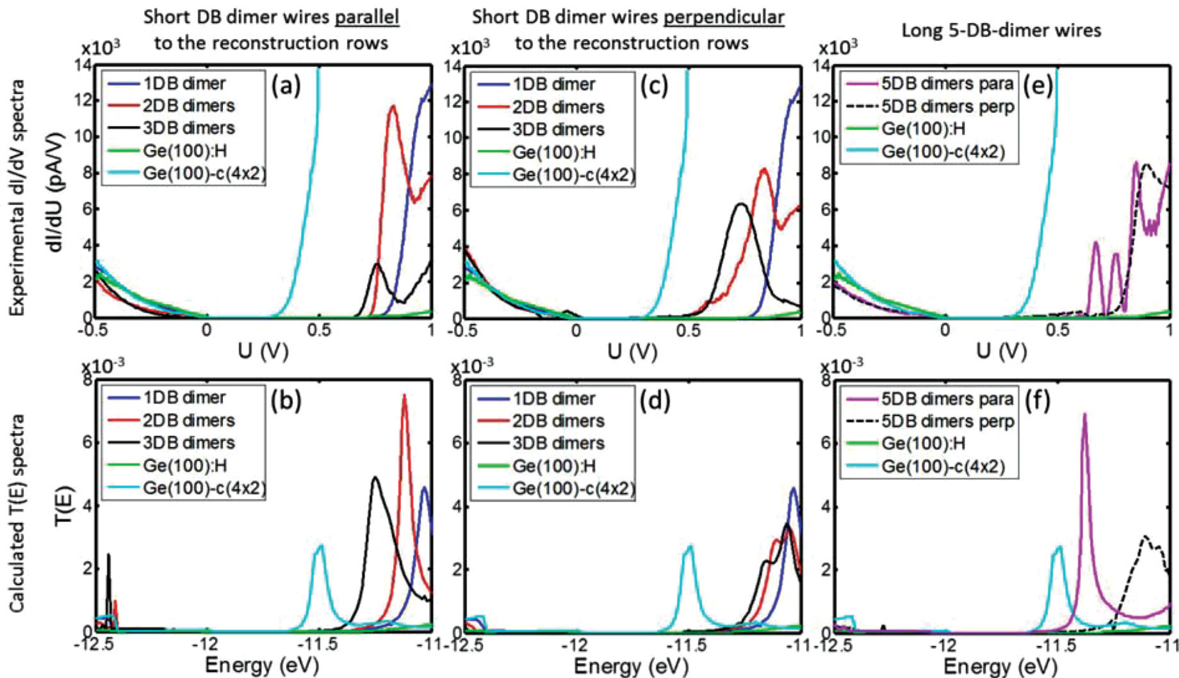

FIG. 4. (Color online) (a), (c), and (e) Experimental dI/dV and (b), (d), and (f) calculated $T(E)$ spectra for a fully hydrogenated Ge(001)-(2×1):H, DB lines containing 1, 2, 3, and 5 DB dimers aligned parallel and perpendicular to the Ge(001):H dimer rows and clean Ge(001) surface with $c(4\times2)$ reconstruction [STS feedback loop at 0.5 nA and −0.5 V for all cases except for 2 and 3 DB dimers in (a) and 5 DB dimers in (e), where 0.3 nA and −0.5 V setpoint was used].

and an infinitely long DB dimer line results in a dispersive π^* band as shown in Fig. 3(c). For short DB lines composed of 2 and 3 dimers, the dI/dV resonances indeed gradually shift towards lower energies compared to the resonance peak for a single DB dimer [Fig. 4(a), red and black resonances], which is also observed in the calculated $T(E)$ spectra [Fig. 4(b), red and black resonances]. When the number of DB dimers increases to 5, the dI/dV resonances shift further to lower energies [Fig. 4(e), pink resonance], gradually approaching the conduction band edge of the bare Ge(001) surface [Fig. 4(e), light blue resonance]. The $T(E)$ spectra show the same trend [Figs. 4(b) and 4(f)]. For DB lines parallel to the dimer rows, the gradual shift of the resonance peaks results from the significant electronic couplings between the nearest-neighbor DB dimer states [see Appendix B, Figs. 10]. Note that only one resonance is observed in the $T(E)$ spectrum for the 5 DB dimer line [Fig. 4(f), pink resonance], whereas a few peaks are observed in the dI/dV plot [Fig. 4(e)]. This is because the tip position is fixed above the central DB dimer for the $T(E)$ calculation, whereas the dI/dV plot is averaged over the DB line. Since each $T(E)$ peak results from a different DB dimer along the DB line, different peaks are enhanced in the $T(E)$ depending on the tip position. In all cases, no significant shift was observed in the valence band edge.

Similar to DB lines parallel to the dimer rows, the resonance peaks shift to lower energies for lines of 2 and 3 DB dimers perpendicular to the dimer rows. However, the shift in the measured dI/dV spectra is larger than the shift in the calculated $T(E)$ spectra [Figs. 4(c) and 4(d)]. For perpendicular DB lines, the shift in the $T(E)$ resonances due to coupling between DB states is expected to be small because the band structure for an infinite perpendicular DB line shows only a nondispersive π^* band located at the edge of Ge(001):H conduction band [Fig. 3(b)]. This difference between the measured and calculated shifts, however, results from a competition between surface atomic structure relaxation towards their infinite configurations and interdimer electronic interactions along those DB lines. Since the interdimer distance is larger for a perpendicular DB line, the buckling of the dimers for short 2 and 3 DB dimer lines is more flexible than for short parallel DB lines. For example, when the buckling of the perpendicular DB dimers is reduced by 25%, the DB-derived states shift down by almost 0.1 eV, and show a resonance shift similar to the one observed in the dI/dV spectra [Fig. 4(c)]. This flexibility hence causes the dI/dV shifts for short perpendicular DB lines to be similar to those observed for short parallel DB lines. However, when the length of the perpendicular DB line exceeds 3 DB dimers, the buckling becomes less flexible and approaches the buckling for the infinite DB line. Therefore, when the number of DB dimers is increased to 5, the resonance peak in both the dI/dV and the $T(E)$ spectra shifts up in energy, and becomes close to the position for a single DB dimer [dashed black resonance, Figs. 4(e) and 4(f)]. This behavior is very different from the trend observed for the parallel DB line with 5 DB dimers.

IV. CONCLUSIONS

In conclusion, we have developed an efficient protocol to construct atomically precise DB nanostructures on a Ge(001):H platform, by selective dimer-by-dimer hydrogen desorption. Unlike on Si(001):H, the DB states on Ge(001):H can be characterized by STS methods on an undoped substrate. Comparison of first-principles calculations with high-resolution STM images confirms that the DB dimers are stabilized in buckled configurations, in contrast to isolated DBs on Si(001):H. The creation and gradual shift of DB electronic states as a function of the number of DB dimers has been probed by STS measurements. We demonstrate experimentally that the DB electronic states are introduced in the Ge(001):H gap differently for DB lines running perpendicular and parallel to the surface reconstruction rows. DB lines parallel to the surface reconstruction rows display a stronger inter-DB dimer electronic coupling, resulting in a dispersive conduction band spanning 0.7 eV for an infinite parallel DB line. Surprisingly, the DB states show similar shifts for short DB lines regardless of their orientation, which can be explained by different physics. For DB lines parallel to the dimer rows, the shift is caused by electronic coupling between neighboring DB dimer states, while for perpendicular DB lines, the corresponding shift results from the more flexible buckling of the DB dimers. This is confirmed spectroscopically for longer perpendicular DB lines, where the DB-derived peak shifts back to a higher energy when the DB buckling settles, while for parallel DB lines the peak continues to shift towards lower energies until the coupling saturates and the full range of the band structure is covered. The presence of states in the Ge(001):H surface band gap together with the ability to split them in both surface directions for 2 and 3 DB dimers provides a powerful tool to build surface atomic-scale logic gates with a minimum number of DBs. Indeed, one can play with those dimer states which, as we have shown, are also interacting in the case of short (3 DB dimers) perpendicular lines.[2] The best approach to interconnect those gates is to construct DB dimer lines parallel to the Ge(001):H rows and to apply a bias voltage higher than + 0.5 V to access the new π^* surface conduction states. The electronic behavior of short DB lines in both directions is of great importance for the design of DB quantum Hamiltonian atomic-scale logic gates, which up to now had only been accessible on a single molecule basis. Furthermore, we have demonstrated that by varying the number of neighboring DBs, the new electronic states located within the intrinsic band gap of the hydrogenated surface can be tuned, which can be utilized to control the charge state of DB quantum dots.

ACKNOWLEDGMENTS

This research was supported by the 7th Framework Programme of the European Union Collaborative Project ICT (Information and Communication Technologies) "Atomic Scale and Single Molecule Logic Gate Technologies" (ATMOL), Contract No. FP7-270028 and by the Visiting Investigatorship Programme "Atomic scale Technology Project" from the Agency of Science, Technology, and Research (A∗STAR). The experimental part of the research was carried out with equipment purchased with financial support from the European Regional Development Fund in the framework of the Polish Innovation Economy Operational Program (Contract No. POIG.02.01.00-12-023/08).

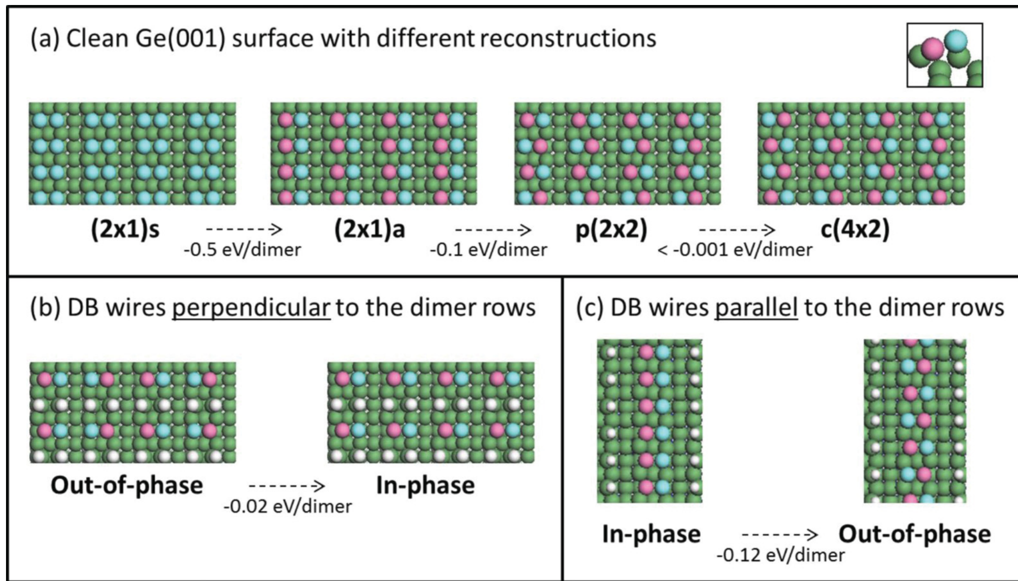

FIG. 5. (Color online) Atomic structure and stability of (a) four different surface reconstruction of Ge(001): $(2 \times 1)s$, $(2 \times 1)a$, $p(2 \times 2)$, and $c(4{\times}2)$, (b) two different buckling configurations for the DB wire perpendicular to the dimer rows, and (c) two different buckling configurations for the DB wire parallel to the dimer rows.

APPENDIX A

Four possible surface reconstructions for Ge(001) are shown in Fig. 5. Among the different surface reconstructions, the most stable reconstruction is $c(4{\times}2)$, but since the difference in energy between $c(4{\times}2)$ and $p(2{\times}2)$ is very small, it is expected that both reconstructions will be observed in the experimental STM image of a clean Ge(001) surface. When the Ge(001) surface is fully hydrogenated, the Ge(001):H surface dimers are symmetric with one H atom per Ge atom. For the DB

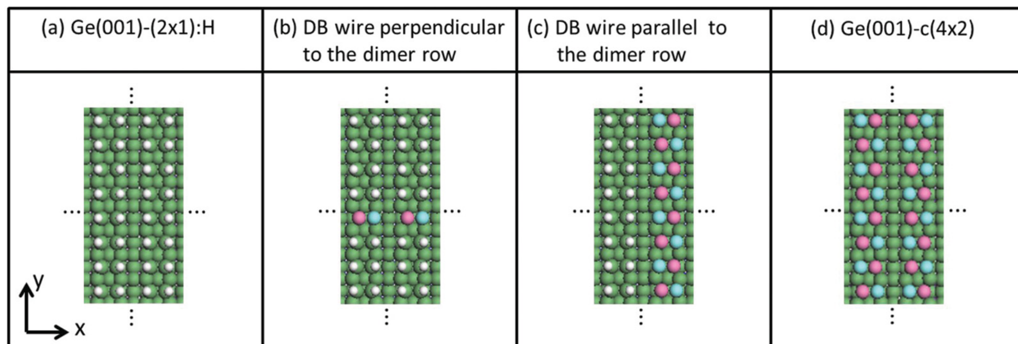

FIG. 6. (Color online) The surface atomic structures used in the band structure calculations shown in Fig. 3.

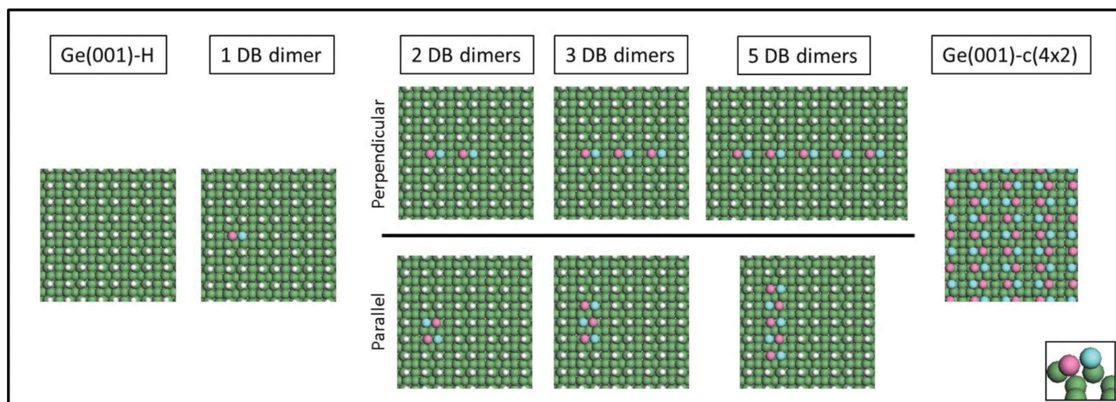

FIG. 7. (Color online) The surface atomic structures used in the image calculations [Fig. 2] and $T(E)$ spectra [Fig. 4].

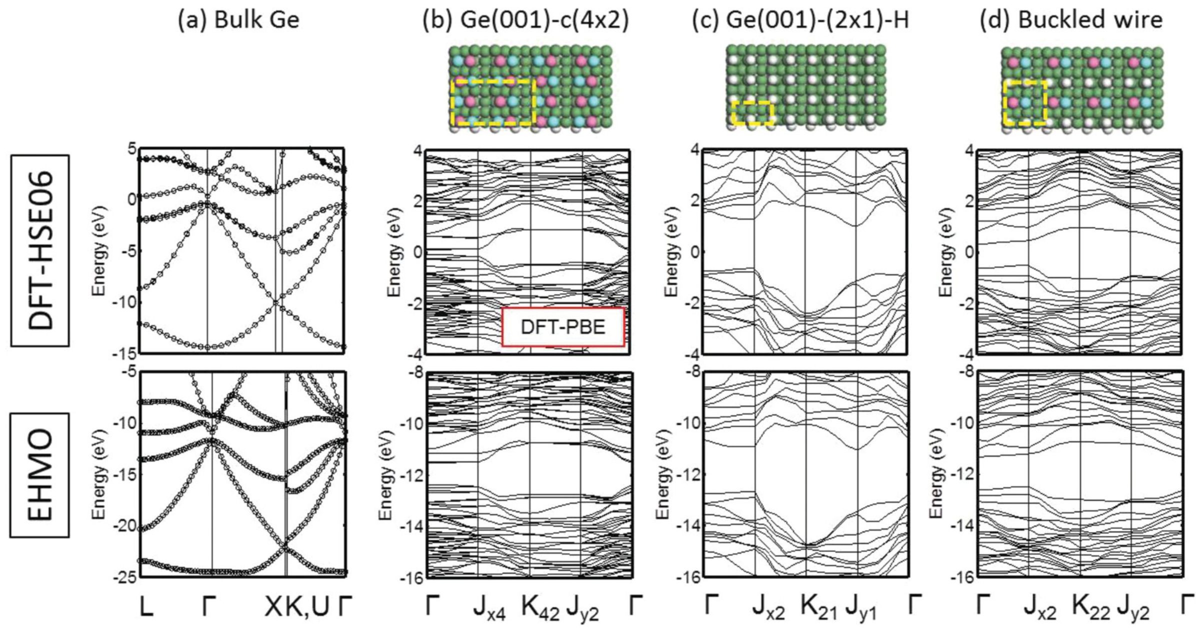

FIG. 8. (Color online) DFT-HSE06 (top row) and EHMO (bottom row) band structures for (a) bulk Ge, (b) Ge(001)-$c(4\times2)$, (c) Ge(001)-(2×1):H, and (d) Ge(001)-(2×1):H surface with buckled wire perpendicular to the dimer rows. The Brillouin zone for each band structure is indicated by the dashed lines on the atomic structure.

wire perpendicular to the dimer rows, the in-phase buckling configuration is slightly more stable than the out-of-phase configuration, but due to the small difference in stability (0.02 eV/dimer), both configurations were observed in STM measurements [Fig. 5(b)]. For the DB wire parallel to the dimer rows, the out-of-phase buckling configuration is more stable than the in-phase configuration by 0.12 eV/dimer, consistent with the energy difference between the $(2\times1)a$ and the $p(2\times2)$ reconstruction [Fig. 5(c)].

The surface atomic structures for the band structures in Fig. 3 are shown in Fig. 6. The same (4×8) unit cell was used for all band structure calculations to allow direct comparison.

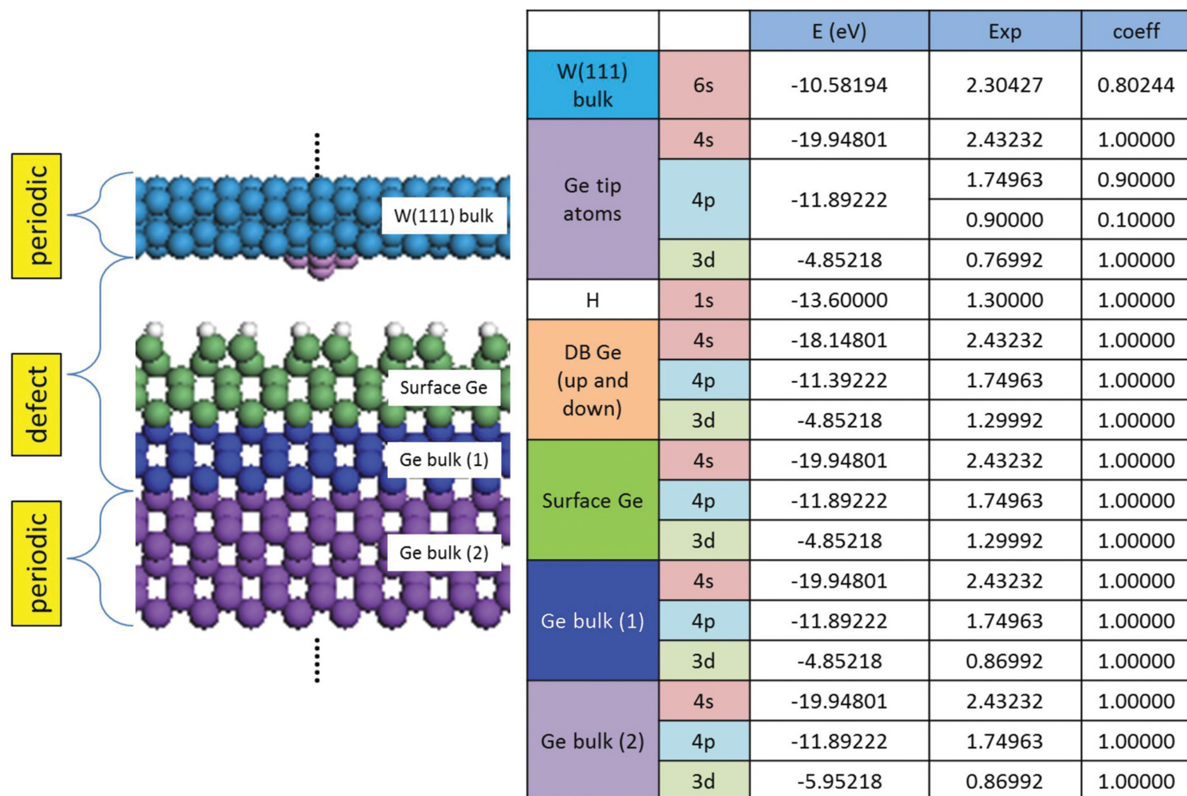

		E (eV)	Exp	coeff
W(111) bulk	6s	-10.58194	2.30427	0.80244
Ge tip atoms	4s	-19.94801	2.43232	1.00000
	4p	-11.89222	1.74963	0.90000
			0.90000	0.10000
	3d	-4.85218	0.76992	1.00000
H	1s	-13.60000	1.30000	1.00000
DB Ge (up and down)	4s	-18.14801	2.43232	1.00000
	4p	-11.39222	1.74963	1.00000
	3d	-4.85218	1.29992	1.00000
Surface Ge	4s	-19.94801	2.43232	1.00000
	4p	-11.89222	1.74963	1.00000
	3d	-4.85218	1.29992	1.00000
Ge bulk (1)	4s	-19.94801	2.43232	1.00000
	4p	-11.89222	1.74963	1.00000
	3d	-4.85218	0.86992	1.00000
Ge bulk (2)	4s	-19.94801	2.43232	1.00000
	4p	-11.89222	1.74963	1.00000
	3d	-5.95218	0.86992	1.00000

FIG. 9. (Color online) The atomic configuration and EHMO parameters used in the STM image and $T(E)$ calculations.

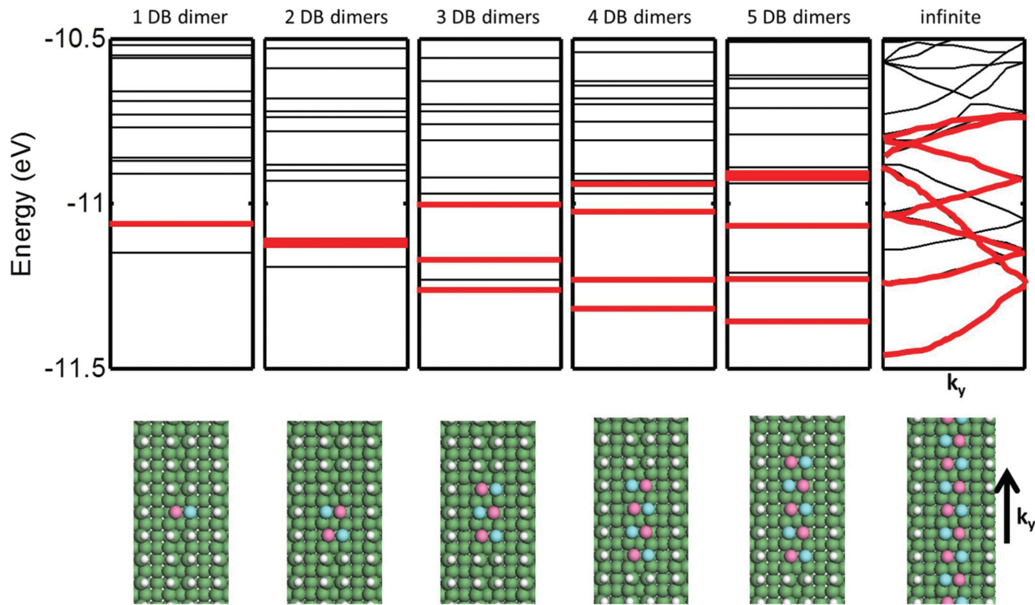

FIG. 10. (Color online) Energy spectra (Γ point) showing the DB states (red lines) for 1, 2, 3, 4, and 5 DB dimers parallel to the dimer rows. The band structure for an infinite line of DB dimers parallel to the dimer rows (k_y) is also shown for comparison.

The surface atomic structures of the calculated images in Fig. 2 and $T(E)$ spectra in Fig. 4 are also shown [Fig. 7]. As mentioned in Sec. II, the parameters in the EHMO Hamiltonian used in the STM image and $T(E)$ calculations were fitted to DFT-HSE06 band structures. In Fig. 8, the DFT-HSE06 and fitted EHMO band structures for bulk Ge and different Ge surfaces are compared, showing the reasonable agreement. Note that the DFT-PBE instead of DFT-HSE06 was used for $c(4 \times 2)$ configuration due to the computational limitation. The atomic configuration and EHMO parameters used in the STM image and $T(E)$ calculations are shown in Fig. 9.

APPENDIX B

As the number of DBs increases, the number of DB states near the conduction band edge increases, and they are dispersed due to the coupling between the DB dimer states. The range of the states for a short line of DBs parallel to the dimer rows eventually evolves to a band as the DB line becomes infinitely long [Fig. 10]. For a line of DBs perpendicular to the dimer rows, the dispersion of the DB states is much smaller than for the parallel direction [Fig. 11].

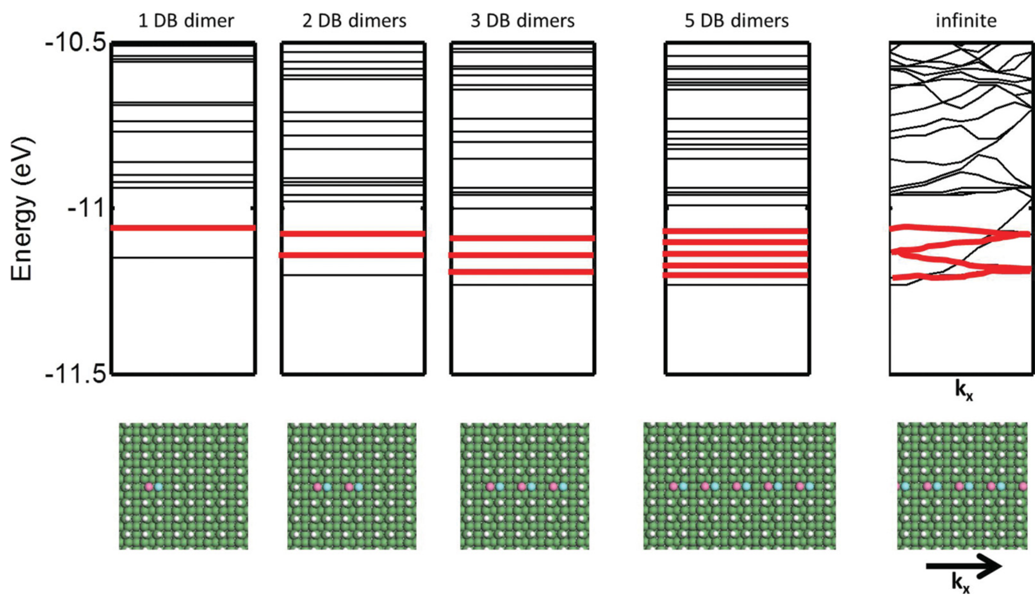

FIG. 11. (Color online) Energy spectra (Γ point) showing the DB states (red lines) for 1, 2, 3, and 5 DB dimers perpendicular to the dimer rows. The band structure for an infinite line of DB dimers perpendicular to the dimer rows (k_x) is also shown for comparison.

*szymon.godlewski@uj.edu.pl
†kawaih@imre.a-star.edu.sg

[1] M. Fuechsle, S. Mahapatra, F. A. Zwanenburg, M. Friesen, M. A. Eriksson, and M. Y. Simmons, Nat. Nanotechnol. **5**, 502 (2010).
[2] H. Kawai, F. Ample, Q. Wang, Y. K. Yeo, M. Saeys, and C. Joachim, J. Phys.: Condens. Matter **24**, 095011 (2012).
[3] L. Soukiassian, A. J. Mayne, M. Carbone, and G. Dujardin, Surf. Sci. **528**, 121 (2003).
[4] T. Hitosugi, S. Heike, T. Onogi, T. Hashizume, S. Watanabe, Z. Q. Li, K. Ohno, Y. Kawazoe, T. Hasegawa, and K. Kitazawa, Phys. Rev. Lett. **82**, 4034 (1999).
[5] B. Weber, S. Mahapatra, H. Ryu, S. Lee, A. Fuhrer, T. C. G. Reusch, D. L. Thompson, W. C. T. Lee, G. Klimeck, L. C. L. Hollenberg, and M. Y. Simmons, Science **25**, 64 (2012).
[6] M. B. Haider, J. L. Pitters, G. A. DiLabio, L. Livadaru, J. Y. Mutus, and R. A. Wolkow, Phys. Rev. Lett. **102**, 046805 (2009).
[7] J. L. Pitters, I. A. Dogel, and R. A. Wolkow, ACS Nano **5**, 1984 (2011).
[8] J. L. Pitters, L. Livadaru, M. B. Haider, and R. A. Wolkow, J. Chem. Phys. **134**, 064712 (2011).
[9] F. Ample, I. Duchemin, M. Hliwa, and C. Joachim, J. Phys.: Condens. Matter **23**, 125303 (2011).
[10] A. Bellec, F. Ample, D. Riedel, G. Dujardin, and C. Joachim, Nano Lett. **9**, 144 (2009).
[11] A. Bellec, D. Riedel, G. Dujardin, O. Boudrioua, L. Chaput, L. Stauffer, and P. Sonnet, Phys. Rev. Lett. **105**, 048302 (2010).
[12] A. Bellec, D. Riedel, G. Dujardin, O. Boudrioua, L. Chaput, L. Stauffer, and P. Sonnet, Phys. Rev. B **80**, 245434 (2009).
[13] T. Hitosugi, T. Hashizume, S. Heike, H. Kajiyama, Y. Wada, S. Watanabe, T. Hasegawa, and K. Kitazawa, Appl. Surf. Sci. **130**, 340 (1998).
[14] J. J. Boland, Phys. Rev. Lett. **67**, 1539 (1991).
[15] D. Chen and J. J. Boland, Phys. Rev. B **65**, 165336 (2002).
[16] K. Bobrov, G. Comtet, G. Dujardin, and L. Hellner, Phys. Rev. Lett. **86**, 2633 (2001).
[17] L. Soukiassian, A. J. Mayne, M. Carbone, and G. Dujardin, Phys. Rev. B **68**, 035303 (2003).
[18] T. C. Shen, C. Wang, G. C. Abeln, J. R. Tucker, J. W. Lyding, and P. Avouris, Science **268**, 1590 (1995).
[19] E. T. Foley, A. F. Kam, J. W. Lyding, and P. Avouris, Phys. Rev. Lett. **80**, 1336 (1998).
[20] G. Scappucci, G. Capellini, W. C. T. Lee, and M. Y. Simmons, Nanotechnology **20**, 495302 (2009).
[21] G. Scappucci, G. Capellini, B. Johnston, W. M. Klesse, J. A. Miwa, and M. Y. Simmons, Nano Lett. **11**, 2272 (2011).
[22] A. Fuhrer, M. Fuechsle, T. C. G. Reusch, B. Weber, and M. Y. Simmons, Nano Lett. **9**, 707 (2009).
[23] S. Watanabe, Y. A. Ono, T. Hashizume, and Y. Wada, Phys. Rev. B **54**, R17308 (1996).
[24] H. Kawai, Y. K. Yeo, M. Saeys, and C. Joachim, Phys. Rev. B **81**, 195316 (2010).
[25] J. Cerda, M. A. Van Hove, P. Sautet, and M. Salmeron, Phys. Rev. B **56**, 15885 (1997).
[26] G. Kresse and J. Hafner, Phys. Rev. B **47**, 558 (1993).
[27] J. P. Perdew, K. Burke, and M. Ernzerhof, Phys. Rev. Lett. **77**, 3865 (1996).